Eur. Phys. J. E **4**, 69–76 (2001)

THE EUROPEAN PHYSICAL JOURNAL E

EDP Sciences

Stability of thin polymer films on a corrugated substrate

N. Rehse, C. Wang, M. Hund, M. Geoghegan[a], R. Magerle, and G. Krausch[b]

Lehrstuhl für Physikalische Chemie II and Bayreuther Zentrum für Kolloide und Grenzflächen (BZKG), Universität Bayreuth, D-95440 Bayreuth, Germany

Received 6 April 2000 and Received in final form 24 August 2000

Abstract. We study the wetting behaviour of thin polystyrene (PS) films on regularly corrugated silicon substrates. Below a critical film thickness the PS films are unstable and dewet the substrates. The dewetting process leads to the formation of nanoscopic PS channels filling the grooves of the corrugated substrates. Films thicker than the critical thickness appear stable and follow the underlying corrugation pattern. The critical thickness is found to scale with the radius of gyration of the unperturbed polymer chains.

PACS. 68.45.Gd Wetting – 68.15.+e Liquid thin films – 61.41.+e Polymers, elastomers, and plastics

1 Introduction

The stability of thin liquid films on solid substrates is an area of great current interest [1–11]. Aside from its technological importance (coatings, lubricants, etc.) there remain various basic issues related to the underlying mechanisms and the relevant forces involved. Since any real surface tends to exhibit both heterogeneities in chemical composition and a certain degree of roughness, recent studies have focussed on the wetting behaviour of heterogeneous model surfaces [5,12–14]. Such surfaces are typically characterised by a well-defined lateral variation of the surface energy and/or a regular corrugation of well-defined shape, depth, and lateral width. In addition to their importance for a sound understanding of the wetting behaviour of real surfaces, such model experiments have demonstrated routes to create liquid microstructures [4,12], which may be of interest for the manipulation of the smallest amounts of liquids in chemical or biochemical applications. In many of the studies referred to above, high molecular weight polymers have played an important role as model liquids. Both the negligible vapour pressure and the high viscosity of polymers facilitate experimental studies of wetting and dewetting because the relevant time scales give easy access to real-time observation of kinetic processes. Furthermore, both the viscosity and the molecular size can be easily controlled by changing the degree of polymerisation, without significantly influencing the surface and interfacial energies involved.

Patterned model substrates have been prepared following different routes. In order to produce micron scale surface energy patterns, different types of lithography have been applied [4,15,16]. As a rule, the overall lateral dimensions of the patterned area created using such techniques decrease with decreasing pattern size. Alternatively, self-assembly processes can be utilised with the potential to create patterns of nanoscopic characteristic lengths over macroscopically large areas. As an example, Mayes and co-workers [17] have used mis-oriented silicon single crystals to produce large areas of saw-tooth like surface morphologies (Fig. 1). Here, a characteristic lateral spacing of order 100 nm can easily be achieved over cm^2-sized surface areas. The authors studied the microdomain morphology of symmetric diblock copolymer thin films of laterally varying film thickness induced by the surface morphology of the substrate. Russell and co-workers [18] introduced the idea of glancing angle metal evaporation on such silicon surfaces, leading to a regular chemical heterogeneity by shadowing effects. On such surfaces they studied the wetting behaviour of thin films of homopolymers, polymer blends, and block copolymers.

In the present paper, we have investigated in detail the stability of thin polystyrene (PS) films of varying molecular weight on regularly grooved silicon surfaces without chemical heterogeneity. We find that the films become unstable below a certain critical thickness t_{crit}, which increases with increasing molecular weight. The data are discussed in view of recent related experiments and theoretical concepts.

2 Experimental

For the preparation of the substrates we used polished silicon wafers ($5 \times 12 \times 0.5\,\mathrm{mm}^3$) with the surface normal pointing $3 \pm 0.5^\circ$ off the $\langle 113 \rangle$ crystal axis towards the $\langle 001 \rangle$ axis (Crystec, Berlin). n-type (arsenic doped) material ($\rho \leq 20\,\mathrm{m}\Omega$ cm) was used to enable resistive heating.

[a] *Present address*: Department of Physics and Astronomy, University of Sheffield, Hounsfield Road, Sheffield S3 7RH, UK. e-mail: mark.geoghegan@sheffield.ac.uk

[b] e-mail: georg.krausch@uni-bayreuth.de

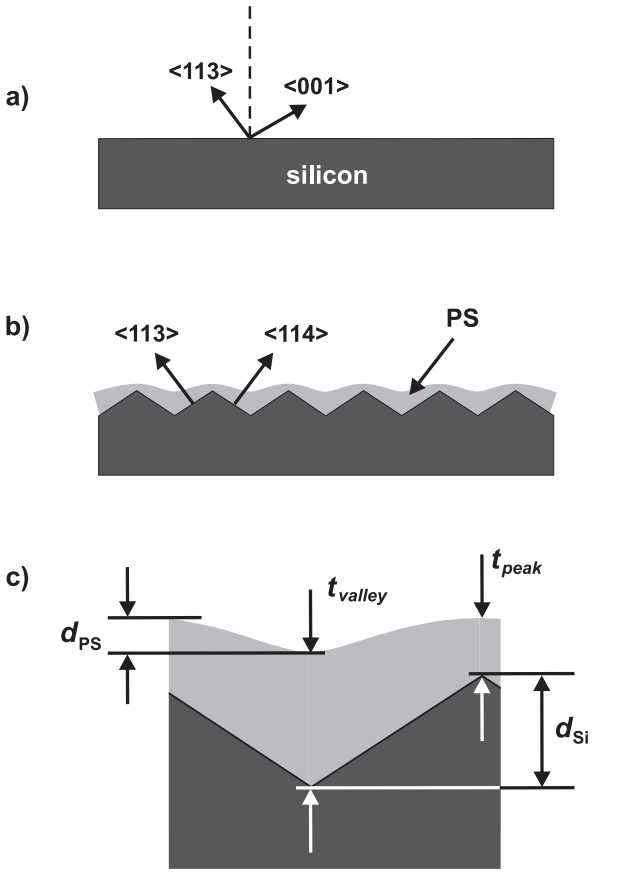

Fig. 1. Sketch of the substrates used in the earlier [17,18] and in the present work. Following the established annealing procedures [19–21], the initially flat surface of the miscut silicon single crystal a) can be transformed into a regularly grooved surface b). A layer of polystyrene is shown in both b) and c). In c) we introduce the respective lengths referred to in the text.

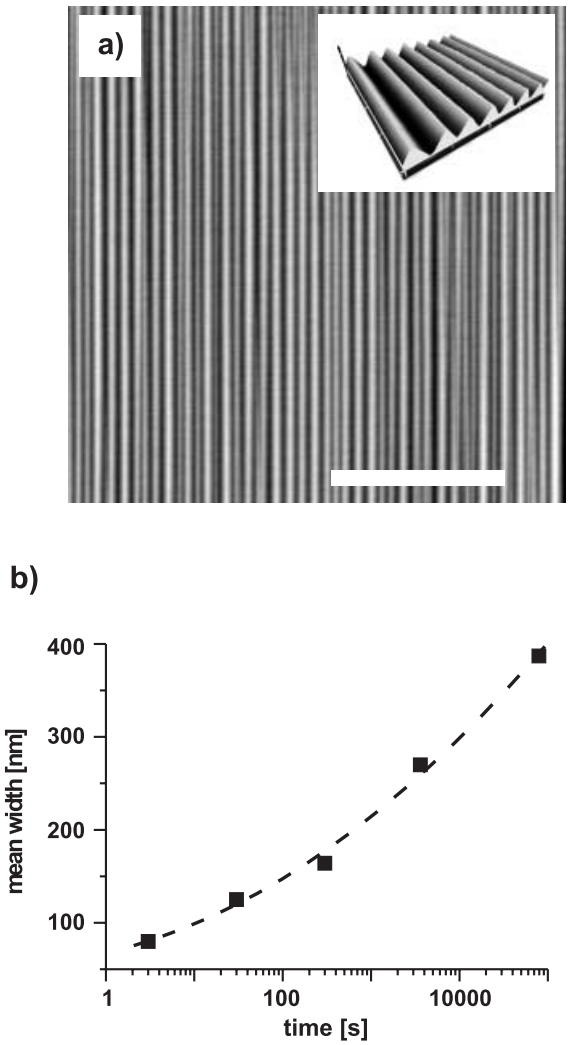

Fig. 2. a) SFM Tapping Mode^{TM} topography image of a corrugated silicon surface used for the wetting experiments. The scale bar is 4 μm. In the inset we show a three-dimensional image of a 2 μm × 2 μm area of the scan. Note that the height scale ($d_{Si} = 5$ nm) and the lateral scales are different, strongly exaggerating the aspect ratio of the surface structure. b) The mean groove width of the corrugated substrates as a function of the annealing time at 800 °C under ultrahigh vacuum. The errors in time correspond to sample cooling and are approximately 5 s. The uncertainty in the mean groove width is of the same size as the symbols. The dashed line is a guide to the eye.

The wafers were repeatedly heated at increasing temperatures up to a maximum of 1250 °C under ultrahigh vacuum conditions. Heating was interrupted whenever the pressure in the vacuum system increased to above 10^{-8} mbar. 25–50 steps were typically needed to remove the native oxide layer under sufficiently high-vacuum conditions. After the last heating step the sample was slowly cooled to temperatures around 800 °C and kept there for various times to produce the grooved surface morphology [19–21]. Finally the wafers were quenched to room temperature and exposed to ambient conditions. The entire heating procedure was computer-controlled. The resulting surface structure was investigated by scanning force microscopy (SFM) operated in TappingMode^{TM}. In Figure 2a we show a typical SFM image taken after a heat treatment at 835 °C for 7 h. The surface exhibits triangularly shaped grooves with a mean width of some 250 nm and a mean peak-to-valley depth d_{Si} of 5 nm. The angle between successive facets is determined by the angle between the (113) and (114) crystallographic planes, respectively (5.8°), resulting in a very shallow grating (Figs. 1b and 2a). We note that the height scale and the lateral scales of the SFM image in the inset to Figure 2a are significantly different, strongly exaggerating the aspect ratio of the grating. The absolute values of the mean groove width and the peak-to-valley depth can be varied over a wide range by suitable choice of annealing time (Fig. 2b) [19–21]. The pattern extends over the entire wafer and the orientation of the grooves is the same over the entire area since it is determined by the macroscopic miscut of the silicon single crystal.

Monodisperse batches of polystyrene of different molecular weights were purchased from Polymer Standards Service, Mainz. The relevant molecular parameters are listed in Table 1. Thin films of PS were prepared by

Table 1. Molecular weights, polydispersities and polymerisation indices of the polystyrenes used in the present work.

M_w (Da)	M_w/M_n	N
5610	1.06	54
18800	1.02	181
51500	1.03	495
100000	1.03	962
376000	1.04	3615
1000000	1.04	9615

spin casting from toluene solution. Different film thicknesses were realised by variation of both PS concentration and spinning speed. Each film was prepared under identical conditions on both a grooved silicon surface and on a flat silicon surface. The latter was used to determine the film thickness. To this end, scratches were applied to the polymer films on the flat silicon wafers and the thickness of the film was determined by SFM relative to the underlying substrate.

The films prepared on the grooved substrates were investigated by SFM after spin casting to check that the film completely wetted the substrate. Furthermore, the average peak-to-valley depth d_{PS} of the PS film was determined and compared to the respective silicon surface in order to check for systematic variations of the PS film thickness on the grating. The same region (to within $\pm 10\,\mu$m) of the substrate was imaged before and after PS deposition in order to avoid possible errors due to small lateral differences in PS film thickness. To check the stability of the films against dewetting, the samples were heated to 150 °C at ambient conditions for various annealing times. (A small number of samples were annealed at 180 °C and these gave the same results as those annealed at 150 °C.) After each annealing step, the samples were investigated by SFM. Care was taken to image the same spot on the sample ($\pm 10\,\mu$m) in order to minimise potential errors due to small lateral variations in the surface structure of the substrates.

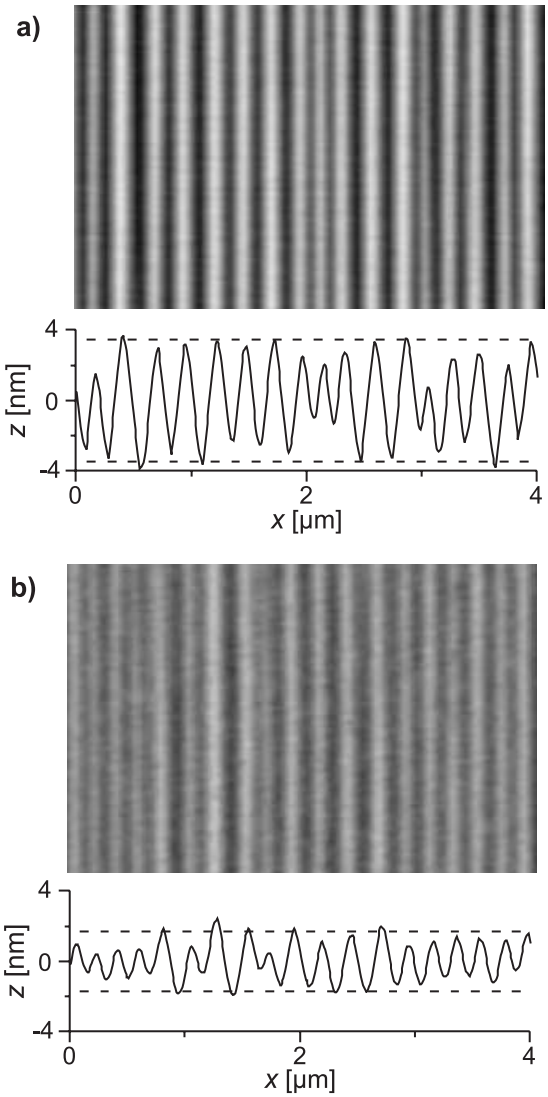

Fig. 3. SFM TappingMode™ topography image of a corrugated silicon substrate before a) and after b) casting a thin PS film ($M_w = 100$ kDa, $t_{av} = 4.5$ nm) from toluene solution. The images have been taken at about the same lateral position of the sample ($\pm 10\,\mu$m). Under each image we show a line scan, averaged along the horizontal direction. The mean square roughness σ_{Si} and σ_{PS} were calculated from the averaged line scans. The dashed lines indicate the respective roughness values.

3 Results

After spin casting, the PS surfaces (Fig. 3b) exhibit qualitatively the same corrugation pattern as the bare Si surfaces (Fig. 3a). This finding shows that homogeneous PS films are formed which follow the underlying grating. For a quantitative analysis of the peak-to-valley depths d_{Si} and d_{PS}, we have averaged the horizontal SFM line scans along the direction parallel to the grooves. The result of this procedure is shown in Figure 3 for a grooved Si surface prior to and after deposition of a 4.5 nm thick layer of PS ($M_w = 100$ kDa). From Figure 3b it is obvious that the peak-to-valley depth of the polymer surface is somewhat smaller than the respective value of the underlying substrate, *i.e.* $d_{PS} < d_{Si}$. This effect is due to the interplay between surface tension and van der Waals interactions, which typically flattens the surface of a polymer film on a rough substrate surface [5,22,23]. Consequently, the film thickness above the peaks, t_{peak} will be somewhat smaller than the thickness in the valleys, t_{valley}. For a quantitative analysis, we determine the root-mean-square roughness σ_i ($i = \mathrm{Si}, \mathrm{PS}$) of the respective surfaces, which, for a perfect triangular grating, is related to the peak-to-valley depths as $d_i = 2\sqrt{3}\sigma_i$. Based on this assumption, we calculate d_{Si} and d_{PS} from the respective roughness data. If the average film thickness is denoted by t_{av}, we can determine $t_{peak} = t_{av} - (1/2)(d_{Si} - d_{PS})$ and $t_{valley} = t_{av} + (1/2)(d_{Si} - d_{PS})$, respectively. For the particular sample shown in Figure 3, we find $t_{av} = 4.5 \pm 0.4$ nm

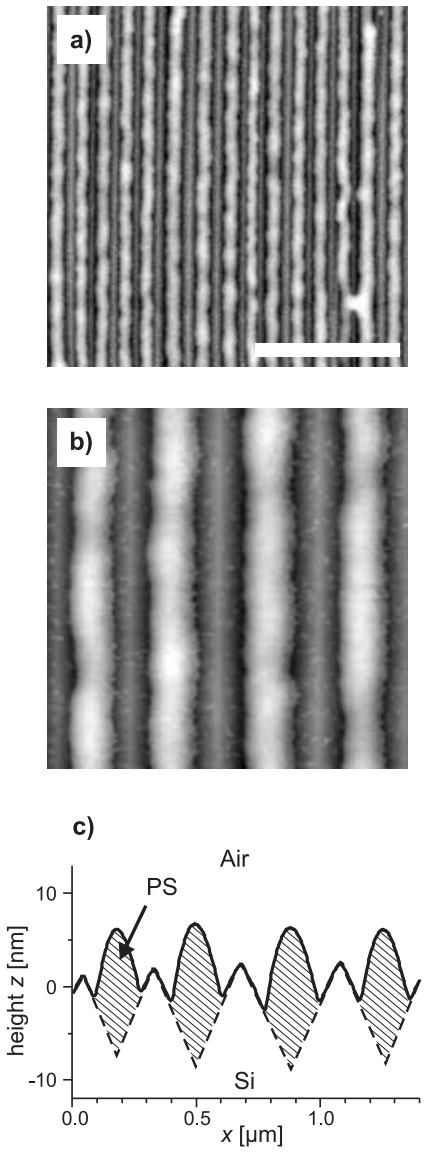

Fig. 4. a) SFM TappingMode^{TM} topography images (the scale bar is $2\,\mu$m) of a thin PS film ($M_w = 100\,$kDa, $t_{av} = 5\,$nm) on a corrugated silicon substrate after annealing at 150 °C for 3 h. The film has broken into linear channels following the grooves of the substrate. The area shown in b) is a $1.5 \times 1.5\,\mu m^2$ scan. c) Average line scan along the horizontal taken from image b). The solid line is the experimental result. The dashed line depicts the position of the substrate surface.

(as determined on a flat substrate), $d_{Si} = 6.9 \pm 0.4\,$nm and $d_{PS} = 3.4 \pm 0.4\,$nm. From these numbers we calculate $t_{peak} = 2.8 \pm 0.5\,$nm and $t_{valley} = 6.3 \pm 0.5\,$nm, respectively.

After annealing, the morphology of the PS film changes markedly. Figure 4 shows the surface morphology of the PS sample discussed above after heat treatment at 150 °C for 3 h. The originally homogeneous film has broken up into thin channels filling the grooves in the underlying Si grating. The channels extend over rather large distances. Further annealing does not alter the film morphology. Figure 4c shows an average line scan similar to the ones displayed in Figure 3. One can clearly see the sharp peaks of the Si grating in between neighbouring PS channels. While the solid line is the experimental result, the dotted line has been added by extrapolation to indicate the position of the PS/Si interface for clarity.

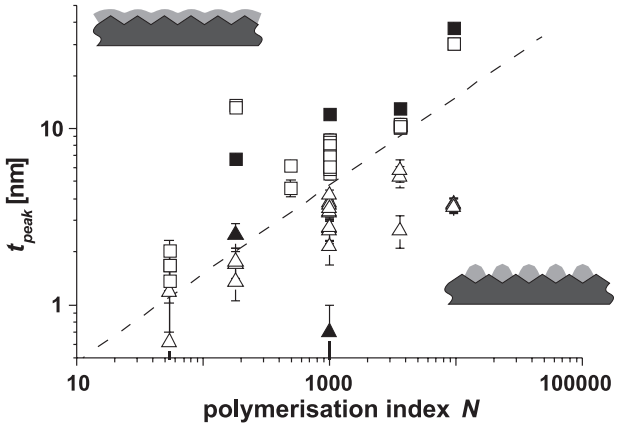

Fig. 5. Summary of the experimental results. Squares indicate stable PS films, while triangles refer to films, where the formation of nano-channels was observed. The dashed line indicates $t_{peak} = 0.55 R_g$. The solid symbols indicate data taken from substrates with no corrugation.

Aiming towards a deeper understanding of the mechanisms responsible for the observed effect, we repeated the above experiment for different film thicknesses t_{av} and different PS polymerisation index N. We find that the PS films break up into a regular array of channels only if the average film thickness is smaller than a critical value, t_{crit}. Films thicker than t_{crit} remain stable even after several days of annealing. The critical film thickness below which the instability is observed increases systematically with increasing chain length. This leads us to infer that the confinement of the chains into films thinner than their radius of gyration ($R_g = 0.67\sqrt{N/6}\,$nm) may be responsible for the observed phenomenon. As the films are thinnest above the peaks of the silicon grating, we present the quantitative results of our study in a double logarithmic plot of t_{peak} against N (Fig. 5). Squares indicate stable PS films, while triangles refer to films which after annealing broke up into channels filling the grooves. The most systematic experiment was performed with $N = 962$ ($M_w = 100\,$kDa), where a clear transition between stable films and PS channels appears at around $t_{peak} = 0.55 R_g$. The data for $N = 3615$ ($M_w = 376\,$kDa) also agree with this relation. For $N = 54$ ($M_w = 5610\,$Da) and $N = 495$ ($M_w = 51.5\,$kDa) stable films were observed for t_{peak} larger but close to $0.55 R_g$, while for $N = 181$ ($M_w = 18.8\,$kDa), PS channels appeared at t_{peak} smaller but close to $0.55 R_g$. All data presented in Figure 5 therefore agree with the notion that films with $t_{peak} > 0.55 R_g$ remain stable while those with $t_{peak} < 0.55 R_g$ break up into channels filling the grooves. We have included the boundary $t_{peak} = 1.50 \pm 0.15 N^{0.5 \pm 0.05}$ ($= 0.55 R_g$) into Figure 5 as a dashed line dividing the diagram into a stable

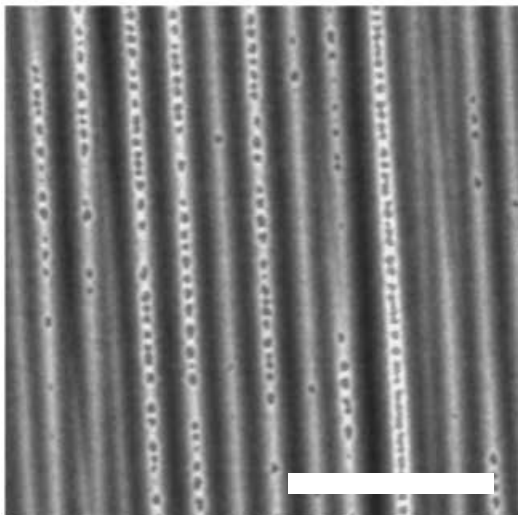

Fig. 6. SFM TappingMode^{TM} topography image of a thin PS film (M_w = 100 kDa, t_{av} = 4.5 nm) after annealing for 3 min at 120 °C. The scale bar is 2 μm.

and an unstable regime. The errors of both the prefactor and the exponent present a range of possible boundaries, which are also compatible with the experimental results.

In order to shed some light on the early stages of the dewetting process finally leading to the observed PS channels, we have performed some preliminary short-time annealing experiments. As an example, Figure 6 shows an SFM image of a 4.5 nm thick PS (M_w = 100 kDa) film after 3 min annealing at 120 °C. The film breaks up by formation of holes lining up above the peaks of the grating. While a systematic study of the time dependence of the dewetting process is beyond the scope of the present paper, the data corroborate the importance of the film thickness t_{peak} for the dewetting behaviour of the films.

The experimental results can be summarised as follows: On chemically homogeneous, grooved silicon substrates, thin PS films break up into channels filling the grooves of the pattern as soon as the film thickness in the thinnest regions above the peaks of the corrugation is smaller than roughly $0.55R_g$. Break-up of the films begins with the formation of holes along the peaks of the corrugation. The resulting PS channels appear stable on further annealing. Thicker films appear to be stable against break-up into channels.

4 Discussion

In general, the free energy of thin polymer films on heterogeneous substrates will exhibit lateral variations. On chemically homogeneous substrates only corrugations need to be considered and the local film thickness is the relevant parameter. As we observe dewetting whenever the thinnest parts of the films are thinner than a critical value $t_{crit} \approx 0.55R_g$, one is led to the issue of chain confinement (the R_g dependence precludes an explanation due to long-range forces). In the following discussion, we therefore consider the potential influence of polymer chain conformation and confinement on the free energy of the films.

To understand the role of chain conformation and confinement in ultrathin polymer films, we need to know whether the chains retain a statistical random walk (Gaussian) distribution near a hard boundary. Silberberg argued that chain conformations remain Gaussian near the surface by assuming that the part of the chain that statistically would want to cross a hard wall is reflected by that wall [24]. This suggests that chains retain their statistical distribution, which in turn means that there is no driving force for a film thickness instability and dewetting. A further development of this theme demonstrated that chain ends induce a long-range repulsion from walls acting over a distance of order R_g, leading to a possible (small) driving force for dewetting [25]. The Silberberg argument has been further criticised in a discussion of computer simulations of thin films confined between neutral walls [26].

We therefore propose that, in confined films, chains will try to reduce distortions induced by the surfaces by moving into thicker regions of the film, triggering dewetting. In thicker films, an increasing number of chains will not be distorted by the boundary surfaces. Since an exchange of undistorted chains between regions of different film thickness does not change the total free energy of the system, films thicker than some critical thickness are expected to remain stable against dewetting. This critical thickness should have a length scale of order R_g. Further support for such a mechanism comes from simulations on the shape of polymer chains in the melt [27]. The chain ends are not located next to each other, and so the polymer chain is actually longer on an axis connecting the chain ends, leading to a cigar conformation for the polymer chain. There is very little change in the polymer size perpendicular to the line joining the chain ends. Therefore, polymers close to hard walls will align themselves such that their long axis is parallel to the wall, avoiding confinement. However, for very thin films of the order of the polymer radius of gyration or thinner, there will be distortions in the chain conformation and dewetting will proceed as described above.

The above argument is also expected to hold on flat substrates. We have therefore performed some test experiments on the stability of ultrathin PS films of different chain length and thickness on flat silicon substrates (Fig. 5). The same substrates were used, with the same preparation procedure. The only difference being that, after annealing at 1250 °C, the substrates were not heated at $\sim$ 800 °C to induce the corrugations. Although a systematic study is beyond the scope of this work, both stable and unstable films were observed. The results support our conclusions for the corrugated substrate experiments.

We note that earlier experiments on the wetting behaviour of ultrathin polymer films [3] on flat substrates showed that otherwise stable films become unstable for thicknesses smaller than some critical value, which again was found to scale as R_g. If films below a certain thickness are indeed inherently unstable, local variations in film

thickness (*e.g.* due to capillary waves) will be amplified, leading to the observed behaviour on flat substrates as well. In the earlier experiments [3] the films were stable at higher temperatures in agreement with the notion of confinement (*i.e.* entropy-related) effects. It has been demonstrated using self-consistent field theory that this dewetting could proceed according to a spinodal mechanism [28]. A systematic study of the role of the annealing temperature in our films could shed light on the importance of such a mechanism.

Recent experiments have addressed the question as to whether the in-plane characteristic dimension of polymer chains changes in films of thickness comparable to or smaller than R_g. While it was generally assumed that within the plane of the films the chains retain their unperturbed Gaussian conformation even in the thin-film limit [24,29], recent experiments lead to contradictory conclusions. Jones *et al.* supported the above assumption by neutron scattering experiments on ultrathin PS films [30]. Other experiments on similar systems indicated a systematic increase of the in-plane dimensions of the chains [31] in ultrathin films in qualitative agreement with simulation results [27]. Experiments on polydimethylsiloxane films coated on PS brushes [32] indicated that chain ordering near a surface occurs. It is probably fair to say that this issue is not yet satisfactorily settled.

In the above discussion we have assumed that the equilibrium conformation of polymer chains in the ultrathin films leads to chain distortion. We cannot, however, exclude the possibility that the preparation of the film leads to the dewetting structure that we observe. For example, during the spin coating, the film can vitrify before all of the solvent has evaporated, possibly leading to some internal tension in the film [33]. In this case one could suppose that the holes formed at the start of the dewetting process (Fig. 6) were nucleated by polymer chain distortions frozen in during spin coating and not due to confinement. Such an explanation is also consistent with the observed effect; the dewetting would be expected to start at the thinnest points on the film (the peaks of the corrugations), and also the radius of gyration scaling of the critical thickness cannot be ruled out under this nucleated mechanism. We therefore only note that significant deformations of the PS chains within the thinnest regions of the films may influence the dependence of the free energy per unit area on film thickness and may be of importance for the effects observed here and in the related experiments [3,18].

The observation of a channel structure initiated by polymer dewetting has been observed in other experiments. Higgins and Jones [34] have shown that an interfacial roughness (of the order of Ångstroms) but with a dominant direction (a kind of nematic roughness) was shown to initiate a corrugated dewetting pattern at a polymer-polymer interface. Such an anisotropic spinodal dewetting at a polymer-polymer interface is probably initiated by small changes in dispersion forces due to the very small differences in film thickness (spinodal dewetting is a very sensitive function of film thickness [2]). The lateral length scale of the dewetting is selected by the polymer system

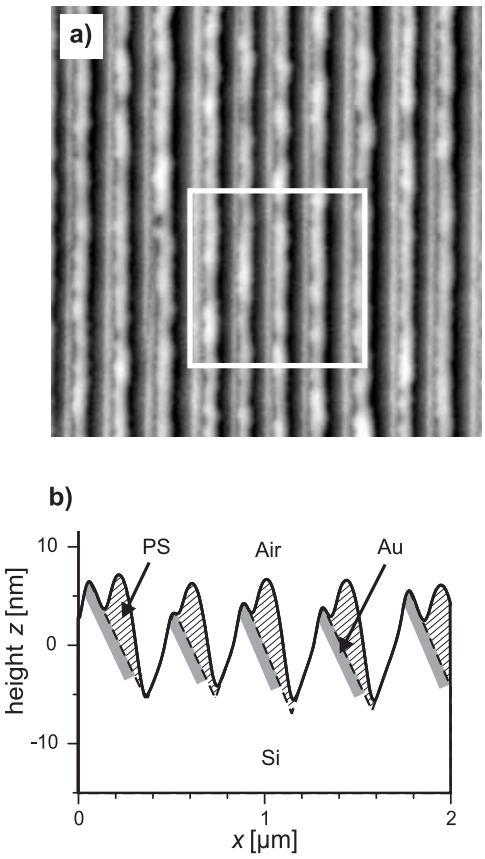

Fig. 7. a) SFM TappingMode^{TM} topography image of a thin PS film (M_w = 100 kDa, t_{av} = 5 nm) on a chemically patterned, corrugated silicon substrate after annealing at 150 °C for 3 h. The film has broken into linear anisotropic channels, with the PS dewetting preferentially to the side of the facet covered with gold. b) Average line scan along the horizontal taken from the area inside the box indicated in image a). The solid line is the experimental result. The dashed line depicts the position of the substrate surface. The approximate location of the gold is sketched on the figure (these SFM measurements do not identify the exact position of the gold).

itself, rather than by the (undefined) size of the roughness. Shorter wavelengths are suppressed due to the energy cost in having a large interface, whilst long wavelengths grow too slowly in comparison with the observed dominant wavelength. This is in contrast to our results, whereby the dewetting has a length scale imposed by the size of the corrugations. The existence of a dominant wavelength is usually associated with a spinodal mechanism, and manifests itself by a wavelength term in the free energy. In order to assess such a possibility in our system, future work should include a detailed analysis of the dewetting of ultrathin polystyrene films on flat substrates.

We end our discussion by noting that the resulting structures observed on the chemically homogeneous, grooved substrates are quite similar to the ones reported by Rockford *et al.* [18], who studied the stability of thin PS films on grooved and chemically patterned substrates. (In these experiments, the mean groove width was 170 nm,

which corresponds to $d_{\mathrm{Si}} \approx 4\,\mathrm{nm}$. Since a 9 nm thick metal layer was evaporated on every other facet, the effective peak-to-valley depth amounted to some 13 nm.) The authors reported a single experiment ($M_{\mathrm{w}} = 100\,\mathrm{kDa}$, $t_{\mathrm{av}} = 5\,\mathrm{nm}$) and showed that the PS film broke up into channels aligned along the grating. They explained their observation by different wetting properties of the SiO_x and Au surfaces, respectively [35]. While the interfacial energy between PS and SiO_x may indeed be larger than for the respective interface with Au [36], our experiments clearly show that no such chemical heterogeneity is needed to induce an instability which finally leads to the formation of PS channels.

To relate our experimental work closer to the situation described by Rockford *et al.* [18], we have in addition prepared grooved silicon surfaces with Au evaporated on every other facet. As an example, Figure 7a shows the morphology of a 5 nm thick PS film ($M_{\mathrm{w}} = 100\,\mathrm{kDa}$) formed on such a chemically heterogeneous substrate after annealing. PS channels are formed, and these are similar to those on the chemically homogeneous, grooved substrates (Fig. 4), although the centre of gravity of the channels is no longer located symmetrically within the grooves. As is clearly visible in the average line scan (Fig. 7b), the PS channels try to cover the facets covered by Au, in agreement with the earlier work [18]. However, we also note that polystyrene has dewetted the very top of the facets. Since gold has also been evaporated onto this part of the substrate, this is clear evidence that the substrate topography must also play a role in such dewetting behaviour.

5 Conclusions

In conclusion, we have demonstrated that a rather small surface corrugation has significant influence on the wetting properties of thin polymer films. In particular, in thin enough films, the spontaneous formation of an ordered array of polymeric nano-channels is observed. The characteristic width of the channels is determined by the corrugation period of the substrate, which can be varied over a rather wide range. The PS films become unstable only if the thickness in the thinnest regions of the films falls beyond a critical value of about $0.55R_{\mathrm{g}}$. It was further suggested that the films dewet by the formation of holes nucleating along the peaks of the corrugation. Given that the substrate corrugation extends over macroscopic areas, this dewetting process leads to a large-scale, highly anisotropic ordered structure.

Films thicker than the critical value of $0.55R_{\mathrm{g}}$ are seen to be stable, probably due to an increasing number of undistorted chains. Such chains do not seek to minimise their free energy by diffusing to thicker areas of the film. In comparison to earlier work on similar, but chemically patterned substrates [18], our results indicate that the roughness itself plays a crucial role in the stability of ultrathin polymer films. Consequently, the potential role of surface roughness should be considered whenever rough surfaces are used to create chemically heterogeneous model surfaces.

The dramatic creation of a macroscopically large ordered array of sub-micron-sized polymer channels induced by a small corrugation in the substrate may inspire further work on the controlled creation of new liquid micro- and nano-structures. We also hope that these results will lead to further experiments aiming to a deeper understanding of the processes involved in the coating of rough surfaces. Furthermore, the results point to the importance of in-depth studies on the chain conformation in ultrathin polymer films and its effect of thin film stability.

The authors appreciate financial support through the Deutsche Forschungsgemeinschaft (Schwerpunkt Benetzung und Strukturbildung an Grenzflächen, Contract No. Kr1369/9). The authors benefited from inspiring discussions with G. Reiter, M. Müller, J.-U. Sommer, R. Seemann, and K. Jacobs.

References

1. P.G. de Gennes, Rev. Mod. Phys. **57**, 827 (1985).
2. F. Brochard-Wyart, J. Daillant, Can. J. Phys. **68**, 1084 (1990).
3. W. Zhao, M.H. Rafailovich, J. Sokolov, L.J. Fetters, R. Plano, M.K. Sanyal, S.K. Sinha, B.B. Sauer, Phys. Rev. Lett. **70**, 1453 (1993).
4. N.L. Abbott, J.P. Folkers, G.M. Whitesides, Science **257**, 1380 (1992).
5. D. Andelman, J.-F. Joanny, M.O. Robbins, Europhys. Lett. **7**, 731 (1988).
6. Y. Liu, M.H. Rafailovich, J. Sokolov, S.A. Schwarz, X. Zhong, A. Eisenberg, E.J. Kramer, B.B. Sauer, S. Satija, Phys. Rev. Lett. **73**, 440 (1994).
7. G. Reiter, Phys. Rev. Lett. **68**, 75 (1992).
8. R. Yerushalmi-Rozen, J. Klein, L.J. Fetters, Science **263**, 793 (1994).
9. G. Reiter, Science **282**, 888 (1998).
10. K. Jacobs, S. Herminghaus, K.R. Mecke, Langmuir **14**, 965 (1998).
11. S. Herminghaus, K. Jacobs, K. Mecke, J. Bischof, A. Fery, M. Ibn-Elhaj, S. Schlagowski, Science **282**, 916 (1998).
12. H. Gau, S. Herminghaus, P. Lenz, R. Lipowsky, Science **283**, 46 (1999).
13. C. Bauer, S. Dietrich, Phys. Rev. E **60**, 6919 (1999).
14. C. Bauer, S. Dietrich, A.O. Parry, Europhys. Lett. **47**, 474 (1999).
15. Y. Xia, X.-M. Zhao, G.M. Whitesides, Microelectr. Engin. **32**, 255 (1996).
16. M. Böltau, S. Walheim, J. Mlynek, G. Krausch, U. Steiner, Nature **391**, 877 (1998).
17. M.J. Fasolka, D.J. Harris, A.M. Mayes, M. Yoon, S.G.J. Mochrie, Phys. Rev. Lett. **79**, 3018 (1997).
18. L. Rockford, Y. Liu, P. Mansky, T.P. Russell, M. Yoon, S.G.J. Mochrie, Phys. Rev. Lett. **82**, 2602 (1999).
19. S. Song, S.G.J. Mochrie, Phys. Rev. Lett. **73**, 995 (1994).
20. S. Song, S.G.J. Mochrie, Phys. Rev. B **51**, 10068 (1995).
21. S. Song, S.G.J. Mochrie, G.P. Stephenson, Phys. Rev. Lett. **74**, 5240 (1995).
22. M.O. Robbins, D. Andelman, J.-F. Joanny, Phys. Rev. A **43**, 4344 (1991).

23. Z. Li, M. Tolan, T. Höhr, D. Kharas, S. Qu, J. Sokolov, M.H. Rafailovich, H. Lorenz, J.P. Kotthaus, J. Wang, S.K. Sinha, A. Gibaud, Macromolecules **31**, 1915 (1998).
24. A. Silberberg, J. Colloid Interface Sci. **90**, 86 (1982).
25. A.N. Semenov, J. Phys. II **6**, 1759 (1996).
26. J.-U. Sommer, A. Hoffmann, A. Blumen, J. Chem. Phys. **111**, 3728 (1999).
27. T. Pakula, J. Chem. Phys. **95**, 4685 (1991).
28. M. Müller, K. Binder, Macromolecules **31**, 8323 (1998).
29. G.J. Fleer, M.A. Cohen-Stuart, J.M.H.M. Scheutjens, T. Cosgrove, B. Vincent, *Polymers at Interfaces* (Chapman & Hall, London, 1993).
30. R.L. Jones, K.S. Kumar, D.L. Ho, R.M. Briber, T.P. Russell, Nature **400**, 146 (1999).
31. A. Brûlet, F. Boué, A. Menelle, J.P. Cotton, Macromolecules **33**, 997 (2000).
32. S. Rivillon, P. Auroy, B. Deloche, Phys. Rev. Lett. **84**, 499 (2000).
33. S. Herminghaus, private communication.
34. A.M. Higgins, R.A.L. Jones, Nature **404**, 476 (2000).
35. R. Konnur, K. Kargupta, A. Sharma, Phys. Rev. Lett. **84**, 931 (2000).
36. T.P. Russell, G. Coulon, V.R. Deline, D.C. Miller, Macromolecules **22**, 4600 (1989).